AD_____

Award Number: DAMD17-98-1-8278

TITLE: Analysis of the Role of Cortactin in Tumor Cell Invasion

PRINCIPAL INVESTIGATOR: Xi Zhan, Ph.D.

CONTRACTING ORGANIZATION: American Red Cross
Rockville, Maryland 20855

REPORT DATE: July 2000

TYPE OF REPORT: Annual

PREPARED FOR: U.S. Army Medical Research and Materiel Command
Fort Detrick, Maryland 21702-5012

DISTRIBUTION STATEMENT: Approved for Public Release;
Distribution Unlimited

The views, opinions and/or findings contained in this report are those of the author(s) and should not be construed as an official Department of the Army position, policy or decision unless so designated by other documentation.

REPORT DOCUMENTATION PAGE

Form Approved
OMB No. 074-0188

1. AGENCY USE ONLY (Leave blank)	2. REPORT DATE	3. REPORT TYPE AND DATES COVERED
	July 2000	Annual (1 Jul 99 - 30 Jun 00)

4. TITLE AND SUBTITLE
Analysis of the Role of Cortactin in Tumor Cell Invasion

5. FUNDING NUMBERS
DAMD17-98-1-8278

6. AUTHOR(S)
Xi Zhan, Ph.D.

7. PERFORMING ORGANIZATION NAME(S) AND ADDRESS(ES)
American Red Cross
Rockville, Maryland 20855

E-MAIL:
zhanx@usa.redcross.org

8. PERFORMING ORGANIZATION REPORT NUMBER

9. SPONSORING / MONITORING AGENCY NAME(S) AND ADDRESS(ES)
U.S. Army Medical Research and Materiel Command
Fort Detrick, Maryland 21702-5012

10. SPONSORING / MONITORING AGENCY REPORT NUMBER

11. SUPPLEMENTARY NOTES

12a. DISTRIBUTION / AVAILABILITY STATEMENT
Approved for public release; distribution unlimited

12b. DISTRIBUTION CODE

13. ABSTRACT *(Maximum 200 Words)*

Cortactin is a prominent substrate of protein tyrosine kinase Src and is frequently amplified and overexpressed along with the chromosome 11q13 in breast cancer [1]. In vitro and in vivo, cortactin binds to and cross-links filamentous actin (F-actin). The F-actin cross-linking activity of cortactin is down-regulated by Src, resulting in increase in dynamics of actin cytoskeleton [2]. We hypothesize that cortactin is implicated in tumorigenesis by promoting metastasis. To test this hypothesis, we developed several retroviruses encoding cortactin variants and infected the viruses into MDA-MB-231 cells. The cells overexpressing wild type cortactin exhibited increase in the motility as analyzed by a Trans-well apparatus, whereas cells overexpressing a cortactin mutant deficient in tyrosine phosphorylation reduced cell motility. We also examined these cells with an in vivo metastasis model in which cortactin overexpressors were injected into the left cardiac ventricle of female nude mice to develop lesions in bone. The preliminary data showed that overexpression of wild-type cortactin increases in metastases of MDA-MB-231 cells in bone and cachexia, whereas cells overexpressing a cortactin mutant deficient in tyrosine phosphorylation showed an impaired capacity to induce osteolytic metastases and cachexia. Furthermore, mice injected with the cells expressing the cortactin mutant tend to have longer life span compared to mice injected with wild-type cortactin transfected cells. These results suggest that tyrosine phosphorylation of cortactin plays an important role in the osteolytic metastases of human breast cancer.

14. SUBJECT TERMS	15. NUMBER OF PAGES
Breast Cancer, Cortactin, Tyrosine Phosphorylation	47
	16. PRICE CODE

17. SECURITY CLASSIFICATION OF REPORT	18. SECURITY CLASSIFICATION OF THIS PAGE	19. SECURITY CLASSIFICATION OF ABSTRACT	20. LIMITATION OF ABSTRACT
Unclassified	Unclassified	Unclassified	Unlimited

NSN 7540-01-280-5500

Standard Form 298 (Rev. 2-89)
Prescribed by ANSI Std. Z39-18
298-102

FOREWORD

Opinions, interpretations, conclusions and recommendations are those of the author and are not necessarily endorsed by the U.S. Army.

_n/a Where copyrighted material is quoted, permission has been obtained to use such material.

_n/a Where material from documents designated for limited distribution is quoted, permission has been obtained to use the material.

_n/a Citations of commercial organizations and trade names in this report do not constitute an official Department of Army endorsement or approval of the products or services of these organizations.

X In conducting research using animals, the investigator(s) adhered to the "Guide for the Care and Use of Laboratory Animals," prepared by the Committee on Care and use of Laboratory Animals of the Institute of Laboratory Resources, national Research Council (NIH Publication No. 86-23, Revised 1985).

N/A For the protection of human subjects, the investigator(s) adhered to policies of applicable Federal Law 45 CFR 46.

N/A In conducting research utilizing recombinant DNA technology, the investigator(s) adhered to current guidelines promulgated by the National Institutes of Health.

N/A In the conduct of research utilizing recombinant DNA, the investigator(s) adhered to the NIH Guidelines for Research Involving Recombinant DNA Molecules.

N/A In the conduct of research involving hazardous organisms, the investigator(s) adhered to the CDC-NIH Guide for Biosafety in Microbiological and Biomedical Laboratories.

7/28/00

PI - Signature Date

Table of Contents

Introduction

Breast cancer is frequently associated with gene amplification at the chromosome 11q13, resulting in overexpression of cortactin, a cortical actin-associated protein and a prominent substrate of protein tyrosine kinase Src *in vivo* and *in vitro*. The protein sequence of cortactin is featured by six tandem copies of a unique 37-amino-acid repeat and a Src homology 3 (SH3) domain at the carboxyl terminus. Between the repeat and the SH3 domain there are an alpha-helical structure followed by a proline-rich sequence. Our previous studies have determined that Src targets either in vitro or in vivo primarily at residues Tyr421, Tyr466 and Tyr482, which locates between the proline-rich and the SH3. In vitro, cortactin binds and cross-links F-actin into meshworks. The F-actin cross-linking activity of cortactin can be dramatically reduced upon tyrosine phosphorylation mediated by Src. The role of Src in the function of cortactin is also implied in the study of Src deficient (Src-/-) cells, in which cortactin fails to respond to FGF-1 for tyrosine phosphorylation and shows less association with polarized lamellipodia at the cell leading edges. In concomitant with low levels of tyrosine phosphorylation of cortactin, Src-/- cells are less motile compared to normal cells and resistant to shape changes induced by FGF-1. These data suggest that tyrosine phosphorylation of cortactin plays an important role in the cytoskeletal reorganization induced by growth factors.

In the present study, we tested hypothesis that cortactin is implicated in tumor metastasis of breast cancer cells. We examined the cells expressing wild-cortactin and $Cort_{F421F466F482}$, which is deficient in tyrosine phosphorylation, in a nude-mice based metastasis assay. Our data shown that overexpression of wild-type cortactin can potentiate metastasis of MDA-MB-231 cells, whereas overexpression of cortactin mutant deficient in tyrosine phosphorylation impaired the metastatic ability of cells in mice.

Body

In the second finding period, we focused on the performance of Task 2, analysis of the effects of cortactin mutants on the invasive ability of tumor cancer cells. The results obtained at the end of this period are summarized follows.

Introduction of retroviruses encoding cortactin variants into MDA-MB-231 cells.
In a previous study, we determined that three major phosphorylation sites at Tyr421, Tyr466 and Tyr482 [3]. To evaluate the role of tyrosine phosphorylation of cortactin in tumor progression, we had tried to transfect cells with cortactin plasmids and analyze stable transfectants selected by G418 in the previous finding period (1998-1999). However, in a more recent study, we found that the selected stable cells had significant variations from clones to clones in either morphology or properties for cell migration and cell growth. To avoid the potential faulty in the interpretation of results, we took a retrovirus-based system in the hope that the infected cells would represent a cell population expressing different levels of cortactin and the results from studying these populations would be more representative.

Retroviruses encoding green fluorescent protein (GFP), GFP-wt-cortactin and GFP-$Cort_{F421F466F482}$, which is deficient in tyrosine phosphorylation [3], was described in an attached manuscript (see Appendix). These viruses were used to infect MDA-MB-231 cells in log phase. Expression of cortactin proteins were verified after two days by immunoblotting with a monoclonal antibody against cortactin. As shown in Figure 1, retroviruses generated a satisfactory efficiency of expression as the levels of GFP-cortactin variants were similar to or slightly higher than those of endogenous cortactin. By flow cytometry analysis, nearly 80% cells were positive for GFP expression (data not shown). The expression of the proteins appeared to be very stable as there were no significant change in the expression after one month (data not shown). When infected cells were exposed to hydrogen peroxide and vanadate (pervanadate), a strong inducer for tyrosine phosphorylation, only endogenous cortactin and GFP-wt-cortactin proteins, but not $Cort_{F421F466F482}$ were phosphorylated, confirming that these three tyrosine residues are essential for phosphorylation [3].

Analysis of cells expressing cortactin variants
The cell populations expressing cortactin variants were first analyzed for the growth capability. As shown in Figure 2, cells expressing cortactin variants exhibited very similar growth rates compared to control cells (cells expressing GFP), confirming the previous notion that cortactin is not directly implicated in the pathway for cell proliferation [4]. Because cortactin is a modulator for actin cytoskeleton, we were more interested in the changes of the motility of cells by analyzing motility of cells using Transwell culture system, a modified Boyden Chamber. As shown in Figure 3, cells expressing GFP-wt-cortactin had about 30% higher motility compared to control cells, whereas cells expressing GFP-$Cort_{F421F466F482}$ were about 20% lower than that of control cells, indicating that GFP-$Cort_{F421F466F482}$ acts as a dominant negative mutant.

The effect of cortactin mutants on the motility of tumor cells in vitro prompted us to examine further the effect of these mutants on tumor metastasis in vivo. We explored a relatively well established metastasis model involving inject cells into nude mice [5]. Briefly, the cells expressing cortactin variants were injected into the left ventricles of BALB/c nude mice. In each group, five mice were examined. To examine the tumor growth in bone tissues, mice were subjected to X-ray photography weekly. Numbers of the tumors, defined by apparent lesions as shown in Figure 4, were countered. As summarized in Figure 5, mice injected with wt-cortactin developed most tumors, about 5 in each animal. In contrast, mice bearing cells expressing cortactin mutant GFP-$Cort_{F421F466F482}$ has least tumors with less one in each mouse. In addition, mice with wt-cortactin expressors were very sick as characterized by small bodies (Figure 4) and were died within six weeks (Figure 6). In contrast, mice bearing cortactin mutants were much healthy compared to both the control group (injected with cells expressing GFP only) and mice injected with wt-cortactin.

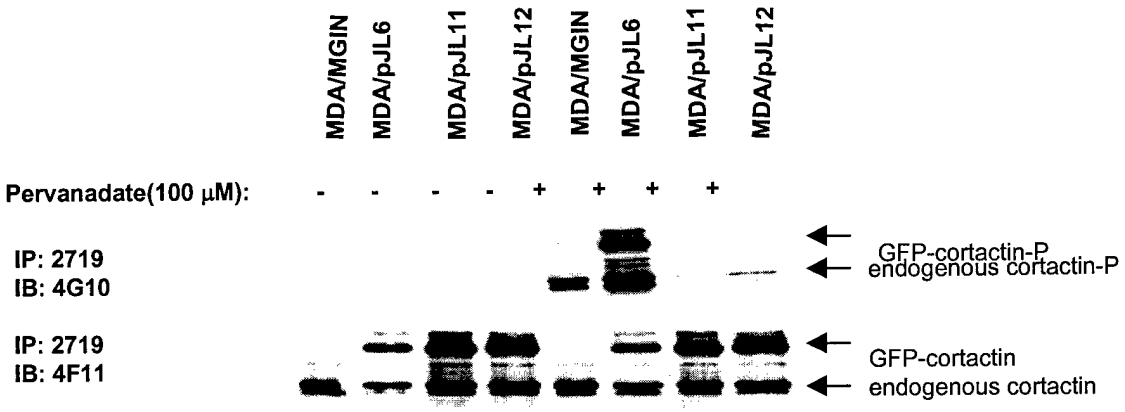

Fig.1. Analysis of tyrosine phosphorylation of GFP-cortactin variants in MDA-MB-231cells. MDA-MB-231 cells were infected with retroviruses encoding GFP-wt-cortactin, GFP-$Cort_{D421D466}$, GFP-$Cort_{F421F466F482}$ and GFP. Infected cells were treated with pervanadate (100 μM) for 45min. The cells were lysed, immunoprecipitated with a cortactin antibody and immunoblotted with a monoclonal phosphotyrosine antibody. The same blot was stripped and re-blotted with a monoclonal cortactin antibody (4F11). The positions for GFP-cortactin and endogenous cortactin were indicated.

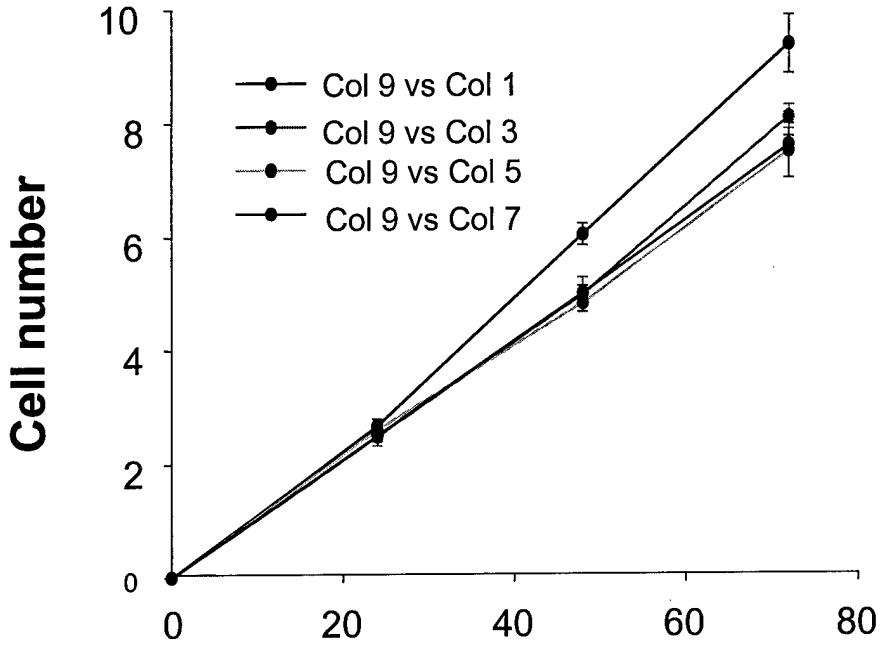

Fig 2. Analysis of growth rate of MDA-MB-231 cells expressing cortactin variants. Cells were plated in a 6-well plate at a density of 105/well in DMEM medium supplemented with 10% of fetal bovine serum and antibiotics. After 24, 48 and 72h, cells were trypsinized and counted using a hemocytometer. The data represented an average of three experiments.

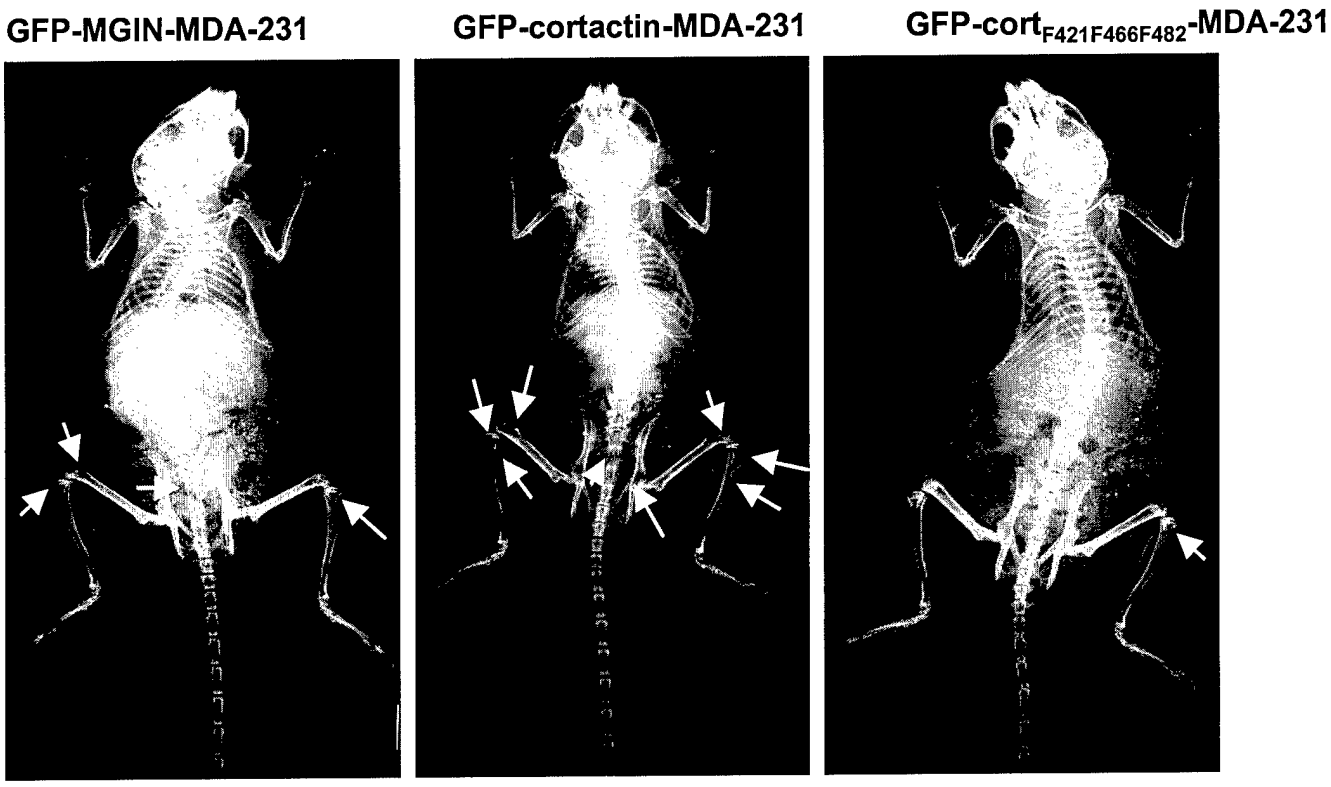

Fig. 4. X-ray autoradiographs of osteolytic lesions in nude mice injected with MDA-MB-231 cells expressing GFP-MGIN, GFP-Cortactin and GFP-Cort$_{F421F466F482}$. Arrows indicate tumors associated with bone. Radiographs were taken 5 weeks after cell inoculation. Note the differences in the number of osteolytic bone metastases between three groups.

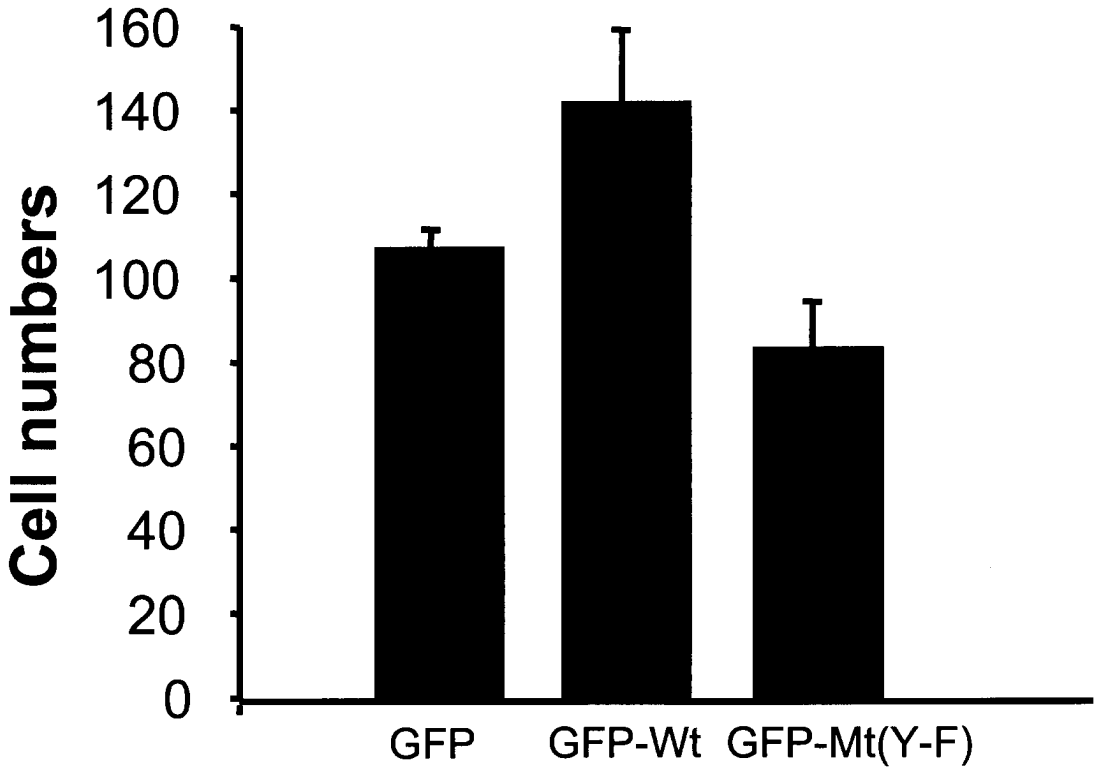

Fig.3 . Analysis of motilities of MDA-MB-231 cells expressing cortactin variants using Transwell apparatus. Cells were plated on the top chambers of a Transwell. Five hours after plating, cells migrated to the lower surface of the filters were countered. The data represent the means with standard derivation of three independent experiments.

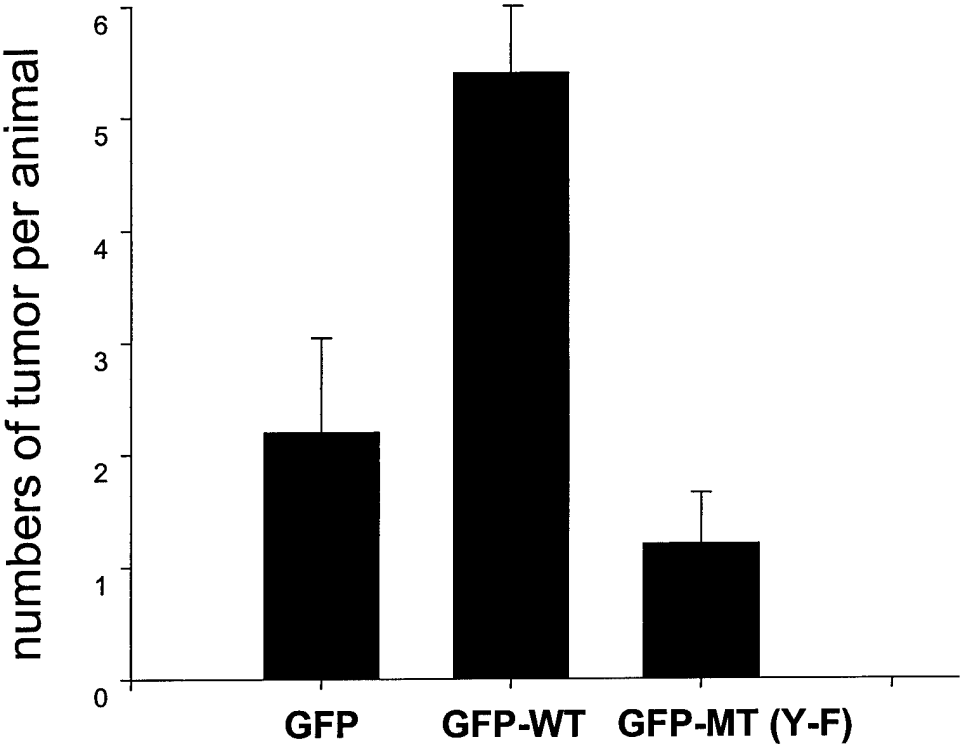

Fig.5. Analysis of the metastatic ability of cells expressing cortactin variants. MDA-MB-231 cells infected with viruses carrying cortactin variants were injected into the left ventricles of nude mice. Five weeks after injection, development of tumors associated with bone tissues were examined with X-ray autoradiography. Data shown are mean±SE (n=5)

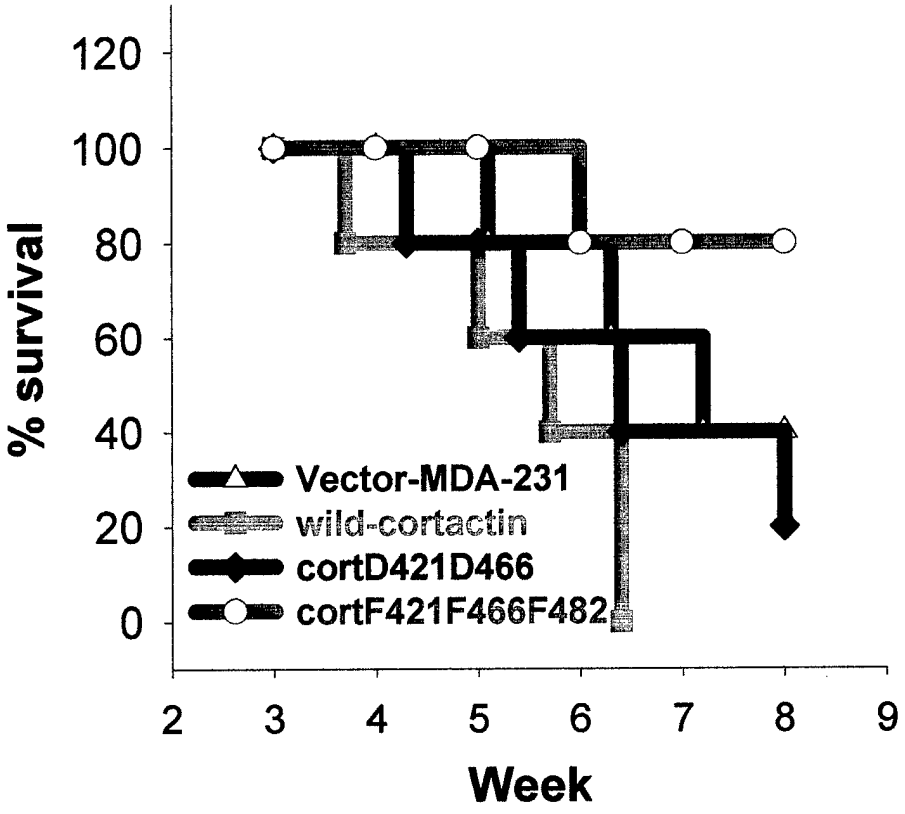

Fig.6. Survival of animals. Nude mice bearing MDA-MB-231 expressing GFP, GFP-wt-cortactin, GFP-CortF421F466F482 and GFP-CortD421D466. Five mice in each group.

Key Research Accomplishments

- Establish retroviruses encoding wild type and mutated forms of cortactin
- Establish MDA-MB-231 cells overexpressing cortactin viruses
- Establish the assays for analyzing tumor cells for cell migration and metastasis
- Demonstrate that wild type cortactin promotes motility of breast tumor cells, whereas mutant form deficient in tyrosine phosphorylation inhibits motility of tumor cells.

Reportable Outcomes

Presentation

Era of Hope Meeting in June of 2000

Manuscripts:

1. Tyrosine Phosphorylation of cortactin is required for H2O2-mediated injury of human endothelial cells. J. Biol. Chem. (in press)

2. Activation of Arp2/3 complex-mediated actin polymerization by cortactin (submitted)

3. The role of tyrosine phosphorylation of cortactin in tumor metastasis (in preparation)

Materials Developments

MDA-MB-231 cells expressing cortactin variants

Conclusion:

Our study has provided first evidence that cells overexpressing wt-cortactin can potentiate metastasis. The function of cortactin in the cell motility appears to require tyrosine phosphorylation as the mutant deficient in tyrosine phosphorylation can inhibit both cell motility in vitro and metastasis in vivo. This study suggests that cortactin can be used as target at which an efficient therapeutic strategy to inhibit metastasis may be developed in the future.

Reference

1. Schuuring, E. D., Verhoeven, E., Litvinov, S., and Michalides, R. J. A. M. (1993) *Mol.Cell Biol.* **13,** 2891-2898

2. Huang, C., Ni, Y., Gao, Y., Wang, T., Haudenschild, C. C., and Zhan, X. (1997) *J.Biol.Chem.* **272,** 13911-13915

3. Huang, C., Liu, J., Haudenschild, C. C., and Zhan, X. (1998) *J.Biol.Chem.* **273,** 25770-25776

4. Liu, J., Huang, C., and Zhan, X. (1999) *Oncogene* **18,** 6700-6706

5. Price, J. E., Polyzos, A., Zhang, R. D., and Daniels, L. M. (1990) *Cancer Res.* **50,** 717-721

APPENDICES

Tyrosine Phosphorylation of Cortactin Is Required for H_2O_2-Mediated Injury of Human Endothelial Cells

Yansong Li, Jiali Liu and Xi Zhan

Department of Experimental Pathology

Holland Laboratory, American Red Cross, 15601 Crabbs Branch Way, Rockville, MD 20855

Telephone: (301) 738-0568

Fax: (301) 738-0879

E-mail: **zhanx@usa.redcross.org**

Key words: H_2O_2, Src, cortactin, endothelial cells, tyrosine phosphorylation and cytoskeleton

Running title: implication of Src and cortactin in jury of endothelial cells

Abbreviations: Erk, extracellular signal-related kinase; F-actin, filamentous actin; FGF, fibroblast growth factor; fluorescein isothiocyanate (FITC); GFP, green fluorescent protein; GST, glutathione S-transferase; HUVE, human umbilical vein endothelial; PCR, polymerase chain reaction; SH3, Src homology 3.

Acknowledgment: We thank Susette Mueller for confocal microscopic analysis, Mehrdad Tondravi for the help of virus preparation and Teresa Hawley for the use of fluorescent cell sorting system. We also thank Takehito Uruno and Peijing Zhang for critical reading. This study was supported in part by National Institutes of Health Grant R01 HL52753-07, US Army grant DAMD17-98-8278 and American Heart Association Established Investigator Grant 0040135N (to X.Z)

ABSTRACT.

Injury of endothelial cells induced by reactive oxygen species plays an important role in the development of early stages of vascular diseases such as hypertension and atherosclerosis. Exposure of human umbilical vein endothelial cells to hydrogen peroxide (H_2O_2), a common form of reaction oxygen species, triggers a series of intracellular events, including actin cytoskeletal reorganization, cytoplasm shrinkage, membrane blebbing and protein tyrosine phosphorylation. The effect of H_2O_2 on endothelial cells is dramatically enhanced when a survival pathway involving extracellular signal-regulated kinase (Erk) is blocked by PD098059. In contrast, the injury of endothelial cells mediated by H_2O_2 is inhibited by PP2, a selective specific inhibitor for protein tyrosine kinase Src. Cortactin, a filamentous actin (F-actin) associated protein, becomes phosphorylated at tyrosine residues upon stimulation by H_2O_2 in a manner dependent on the activity of Src. The level of tyrosine phosphorylation of cortactin is correlated with the formation of membrane blebs. Overexpression of wild-type cortactin conjugated with fluorescent green protein (GFP) in endothelial cells via a retroviral vector substantiates the H_2O_2-induced morphological changes, whereas overexpression of a GFP-cortactin mutant deficient in tyrosine phosphorylation renders endothelial cells resistant to H_2O_2. The functional role of cortactin in H_2O_2-mediated shape changes was also evaluated in NIH 3T3 cells. Stable 3T3 transfectants expressing wild-type cortactin in the presence of either H_2O_2/PD098059 or H_2O_2 alone at 200 μM exhibited a dramatic shape change characterized by rounding up or aggregation. However, the similar changes were not detected with cells overexpressing a cortactin mutant deficient in tyrosine phosphorylation. These data demonstrate an important role of the Src\cortactin-dependent actin reorganization in the injury of endothelial cells mediated by reactive oxygen species.

INTRODUCTION

The injury of endothelial cells underling the lumen of blood vessels contributes significantly to the development of atherosclerosis and hypertension. Numerous studies have shown that exposure to local reactive oxygen species is one of the main causes for the injury of endothelial cells. Reactive oxygen species can be derived from the dismutation of superoxide anion or from the products of activated neutrophils or macrophages that accumulate in the blood vessel wall as a consequence of ischemia and reperfusion injury [1-3]. Cancer cells also produce reactive oxygen species in vivo, which may contribute to the damage of endothelium during the metastatic process [4]. Hydrogen peroxide (H_2O_2) is known to be one of the common forms of reactive oxygen species and can easily penetrate the plasma membrane and affect neighboring cells as well as H_2O_2 producing cells[5]. One of the prominent events within endothelial cells upon exposure to H_2O_2 is the formation of plasma membrane blebs [6]. The surface blebbing of endothelial cells promotes platelets to adhere to the injured endothelium as well as leukocytes to block capillary lumens, which would lead ultimately to cardiac, brain, lung, kidney and liver failure. While the mechanism of the formation of membrane blebs is not fully understood, it appears to be intimately associated with the reorganization of the actin cytoskeleton that are mediated by cytoskeleton binding or cross-linking proteins. For example, cells deficient in an actin filament cross-linking protein, ABP-280, show prolonged blebbing [7]. Similarly, redistribution of filamin, another F-actin cross-linking protein, is one of the early events in H_2O_2-mediated endothelial cell injury [8].

H_2O_2 triggers signal transduction within cells in a similar manner as growth factors [9;10]. Exposure to H_2O_2 induces a rapid increase in tyrosine phosphorylation of a various proteins,

including Src and Syk related non-receptor protein tyrosine kinases [11], and enhances the kinase activity of Src in endothelial cells [12]. The implication of protein tyrosine phosphorylation in H_2O_2-mediated signal transduction is further strengthened by the findings that non-selective tyrosine kinase inhibitors such as genistein and herbimycin A can abolish the response of cells to H_2O_2 [13;14]. In addition to protein tyrosine kinases, H_2O_2 also induces the activity of extracellular signal-regulated kinase (Erk), a member of the mitogen-activated protein kinase (MAPK) family [15]. Induction of Erk may represent a surviving pathway because selective inhibition of Erk by PD098059, can increase apoptosis induced by H_2O_2 [9;16].

Cortactin, a cortical actin-associated protein that is widely expressed in most adherent cells [17], is a prominent substrate of protein tyrosine kinase Src in vivo and in vitro [18;19]. The protein sequence of cortactin is featured by six and half tandem repeats of a unique 37-amino-acid sequence and a Src homology 3 (SH3) domain at the carboxyl terminus. Between the repeat and the SH3 domain there is an alpha-helical structure followed by a proline-rich region. Our previous studies have determined that Src targets cortactin primarily at three residues (Tyr421, Tyr466 and Tyr482) between the proline-rich and the SH3 domain [20]. In vitro, cortactin binds to and cross-links F-actin into meshworks [18]. The F-actin cross-linking activity of cortactin can be dramatically reduced upon tyrosine phosphorylation mediated by Src [18]. The role of Src in the function of cortactin was also appreciated during the study of Src deficient (Src-/-) cells in which cortactin fails to respond to FGF-1 for tyrosine phosphorylation and shows less association with polarized lamellipodia. In concomitant with low levels of tyrosine phosphorylation of cortactin, Src-/- cells are less motile compared to normal cells and resistant to FGF-1-mediated shape changes [19]. These data suggest that tyrosine phosphorylation of cortactin plays an important role in the dynamic change of the actin cytoskeleton induced by growth factors. In the study

presented here, we examined the role of cortactin and Src in the injury of endothelial cells induced by H_2O_2. We found that H_2O_2 induces a significant increase in tyrosine phosphorylation of human endothelial cortactin in a manner dependent on the activity of Src. Furthermore, overexpression of wild-type cortactin enhances the response of endothelial cells to H_2O_2, whereas overexpression of a cortactin mutant deficient in tyrosine phosphorylation significantly reduces the H_2O_2-mediated injury of endothelial cells. Thus, this study demonstrates that the signal pathway involving Src and cortactin is implicated in the injury of endothelial cells.

METHODS AND EXPERIMENTAL PROCEDURES

Reagents

H_2O_2, dimethyl sulfide (DMSO) and heparin were purchased from Sigma Chemical Co. (St. Louis, MO). PP2, SB203580 and PD098059 were from Calbiochem (La Jolla, CA). Lipofectamine and G418 were purchased from Life Technologies Inc. (Rockville, MD). Protein A Sepharose CL-4B and ECL western blotting kits were from Amersham Pharmacia (Piscataway, NJ).

Antibodies

Monoclonal anti-phosphotyrosine antibody (4G10) and monoclonal anti-cortactin antibody 4F11 were purchased from Upstate Biotechnology, Inc. (Lack Placid, NY). Antibodies against Erk (both type 1 and type 2 forms) were from Promega (Madison, Wisconsin). Polyclonal cortactin antibodies were prepared as previously described [21].

Cell culture

Human vein umbilical endothelial (HUVE) cells were purchased from Clonetics (Walkersville, MD). HUVE cells were grown in medium M199 supplemented with 10% (vol/vol) fetal bovine serum (FBS), heparin and human recombinant FGF-1 (10 ng/ml) in cell culture dishes coated with fibronectin (5 $\mu g/cm^2$). Cells with passages less than 15 were used in this study. NIH 3T3 cells and cortactin transfectants were cultured in Dulbecco's modified Eagle's medium (DMEM) (Fisher Scientific, Pittsburgh, PA) supplemented with 10% (vol/vol) calf serum and antibiotics.

Construction and preparation of cortactin viruses

A plasmid encoding green fluorescent protein (GFP)-Cortactin was prepared as following. A DNA fragment encoding cortactin coding sequence was generated by polymerase chain reaction

(PCR) using a cDNA clone encoding murine cortactin as the template 21. The primers used in PCR were CATTGTGTCGACTGGAAAGCCTCTGCA and CATGCTGGATCCCTACTGCCGCAGCTCC. The PCR product was inserted into the Sal1 and BamH1 sites of pEGFP-C1 (Clontech, Palo Alto, CA). The resulting plasmid was named as pJQ-7. The encoding sequence of GFP-cortactin was further inserted into *Age*1 and *Not*1 sites in a retroviral plasmid MGIN (a gift of Robert Hawley, Holland Laboratory). The *Age*1 and *Not*1 sites were introduced with PCR using primers GCGCTACCGGTCGCCACC and ACGTCCGCGGCCGCCTACTGCCGCAGCTC. The final resulting plasmid was named as pJL-6.

To prepare GFP-Cort$_{F421F466F482}$, the sequence spanning the mutation sites in the plasmid pCH17 [18] was amplified with PCR using primers GACAAGAATGCATCCACCTTT and ACGTCCGCGGCCGCCTACTGCCGCAGCTC. The PCR product was inserted into the unique sites *Nsi*I and *Not*1 sites on pJL-6. The resulting plasmid was named as pJL-12.

Preparation of viruses

Retrovirus packaging cells (293GPG) were the gift of Mehrdad Tondravi (Holland Laboratory) and maintained in DMEM supplemented with 10% FBS, 1 mM MEM sodium pyruvate, 2 mM L-glutamine, antibiotics, 1 μg/ml tetracycline, 2 mg/ml puromycin and 0.3 mg/ml G418. Packaging cells (1x 10^6) were transfected with MGIN viruses using Superfect Transfection Reagent (Qiagen Inc., Valencia, CA). Stable transfectants were selected in a G418-containing medium. To harvest viruses, the stable transfectants were grown in DMEM containing 10% FBS, 1 mM sodium pyruvate and 2 mM L-glutamine. The medium of the transfectants was collected at 48, 72 and 96 hours after plating and filtered through a 0.45 μM filter (Gelman Sciences, Ann Harbor, MI). The virus medium was stored at -70°C.

Viral Infection

HUVE cells were plated at density of $1x10^5$ in 35-mm dishes. On the next day, the medium was replaced with 1 ml of viral supernatant containing 8 μg/ml of polybrene. After 24 h of incubation, the culture medium was changed to M199 containing 10% FBS, 10 ng/ml FGF-1 and 10 μg/ml heparin. Expression of GFP proteins was monitored by fluorescent microscopy. To increase the efficiency of infection, the cells were infected with viruses for two or three times.

FACS analysis and sorting

Infected HUEV cells were trypsinized. The suspended cells (2×10^6) were washed one time with PBS supplemented with 2% FBS. The washed cells were then resuspended in PBS plus 2% FBS and sorted in a fluorescent-activated cell sorting system (Beckton Dickinson, Franklin Lakes, NJ) according to light scatter and fluorescence intensity.

Phosphotyrosine Immunoblot Analysis

Cells were extracted in lysis buffer (50 mM Tris-HCl, pH7.4, containing 1% NP-40, 0.25% sodium deoxycholate, 150 mM NaCl, 1 mM EDTA, 1 mM PMSF, 1 μg/ml aprotinin, leupeptin, pepstatin, 2 mM Na_3VO_4 and 1 mM NaF). The extracts were centrifuged at 14,000 x rpm for 10 min at 4°C. The clarified supernatants were immunoprecipitated with polyclonal cortactin antisera 2719 [21]. The immunoprecipitates were resolved in a SDS-polyacrylamide gel electrophoresis (PAGE) (7.5%, w/v), transferred to a nitrocellulose membrane and further blotted with a monoclonal phosphotyrosine antibody (4G10). In some experiments, the blot membrane was stripped and re-blotted with monoclonal cortactin antibody 4F11 as perviously described [22].

Analysis of activated MAP kinases

Cells were lysed in 0.5 ml of 2×SDS sample buffer. The cell lysates were analyzed in 10% SDS-PAGE and transferred to a nitrocellulose membrane. The membrane was blotted with either active Erk antibody or Erk antibody.

Immunofluorescent Microscopy

Cells were plated on glass coverslips pre-coated with fibronectin. After treatment, the cells were fixed with 3.7% formaldehyde and permeabilized with 0.5% Triton X-100 in PBS for 5 min. The permeabilized cells were incubated with a monoclonal cortactin antibody 4F11 at the concentration of 0.2 μg/ml in PBS containing 5% bovine serum albumin for 1 h. The cells were then incubated for 1 h with rhodamine-conjugated goat anti-mouse IgG (Pierce) at the concentration of 5 μg/ml and fluorescein isothiocyanate (FITC)-labeled phalloidin at the concentration of 1 μM. Between each step, three washes with PBS were applied. After staining with antibodies, the cells were mounted on a glass slide and inspected under a laser confocal scanning or fluorescent microscope.

RESULTS

H_2O_2 induces tyrosine phosphorylation of cortactin

In an attempt to study the mechanism by which oxygen radicals induce the injury of endothelial cells, we examined protein tyrosine phosphorylation in human umbilical vein endothelial (HUVE) cells upon exposure to H_2O_2. It has been demonstrated that H_2O_2 induced injury of endothelial cells requires the function of p38, a MAPK-related kinase, and triggers a survival pathway involving Erk [23]. Thus, we examined HUVE cells exposed to H_2O_2 with and without the presence of SB203580 and PD098059, selective inhibitors for p38 and Erk respectively [24 25]. Tyrosine phosphorylation was assessed by phosphotyrosine immunoblot of the total cell lysates prepared from HUVE cells after H_2O_2 treatment. While H_2O_2 alone at the concentration of 200 μM failed to induce a detectable increase in tyrosine phosphorylation, exposure of cells to PD098059 for 1 h prior to H_2O_2 significantly increased levels of several phosphotyrosyl bands ranging from 60 to 200 kDa. However, PD098059 alone had no detectable effect on tyrosine phosphorylation even at concentrations as high as 200 μM (data not shown). Interestingly, SB203580 did not affect significantly protein tyrosine phosphorylation induced by either H_2O_2 plus PD098059 (Figure 1, lane 5) or H_2O_2 alone at high concentrations (data not shown). Therefore, p38, which is known to be important for the cytoskeletal reorganization mediated by H_2O_2 [23], involves likely a pathway either independent on or downstream of protein tyrosine phosphorylation to regulate the cytoskeletal reorganization.

We noticed that H_2O_2 plus PD098059 induced two phosphotyrosyl bands at p80 and p85 kDa (Figure 1, lane 5 and 6), which were similar to cortactin, a prominent substrate of Src [21;26]. Indeed, treatment of cells with PP2, a selective Src inhibitor, abolished the phosphorylation of p80 and p85 (Figure 1, lane 1and 2). Further confirmation of these two bands as cortactin-related

proteins were performed by immunoprecipitation of cell lysates with a cortactin specific antibody followed by phosphotyrosine immunoblotting. As shown in Figure 2A, H_2O_2 alone induced tyrosine phosphorylation of cortactin in a dose dependent manner. The significant increase in tyrosine phosphorylation did not occur until more than 1.6 mM H_2O_2 was applied. However, in the presence of PD098059, tyrosine phosphorylation of cortactin was readily detectable at concentrations of H_2O_2 as low as 50 μM (Figure 2B). H_2O_2 induced cortactin phosphorylation was also time-dependent. The significant increase in the level of phosphotyrosyl cortactin was readily detected at 30 min after treatment and reached to a maximal level at 45 min (Figure 2C).

Tyrosine phosphorylation is required for H_2O_2 induced membrane blebbing

The morphological changes of endothelial cells induced by H_2O_2 were evaluated by confocal microscopical analysis. Cortactin and F-actin were visualized by a rhodamine-conjugated cortactin antibody and FITC-labeled phalloidin respectively. As shown in Figure 3, no significant shape changes were observed when cells exposed to either H_2O_2 alone (Figure 3A, c) or PD098059 alone (data not shown), although careful examination revealed a slight increase in the formation of stress fibers in the cells treated with H_2O_2 alone (Figure 3A, d). In contrast, cells treated with H_2O_2 plus PD098059 showed dramatic shape changes characterized by formation of membrane blebbing and shrank cytoplasm (Figure 3A, e and f). The H_2O_2 induced shape changes appeared to require the activity of Src because these changes did not occur when cells were pre-treated with PP2 (Figure 3A, g and h). The effect of H_2O_2 on the shape changes of HUVE cells was also quantified by measuring the numbers of cells forming membrane blebs and shrank cytoplasm (Figure 3B). Based on these criteria, H_2O_2 alone induced shape changes in 18% of cells, whereas H_2O_2 plus PD098059 was able to induce changes in nearly 45% of cells.

The shape changes were significantly reduced by more than 50% when cells were pre-exposed to PP2.

PD098059 efficiently inhibited the activity of Erk induced by H_2O_2 (Figure 4). Therefore, it raised a possibility that the decrease in the activity of Erk could be responsible for the H_2O_2 induced injury of endothelial cells. Several lines of evidence suggest that this possibility is unlikely. First, the similar shape changes of HUVE cells can be also observed when cells treated with H_2O_2 alone at high concentrations (2 mM), where the increased Erk activity is remained (Figure 4, lane 5). Second, when cells were treated with H_2O_2 at low a concentration (100 μM) plus vanadate, a mixture that can efficiently increase the tyrosine phosphorylation of cortactin and induce shape changes of HUVE cells (data not shown), also efficiently activated Erk (Figure 4, lane 6). Thus, decrease in Erk activity appears to be not necessarily associated with the injury of endothelial cells. It seems that activated Erk can compromise the effect of H_2O_2 only at low concentrations. In contrast, shape changes of endothelial cells are more intimately associated with the increase in tyrosine phosphorylation of cortactin.

Expression of cortactin mutant confer cells resistant to H_2O_2-mediated shape change

To further evaluate the role of tyrosine phosphorylation of cortactin in the injury of endothelial cells, we constructed several retroviruses encoding a green fluorescent protein (GFP) tagged wild-type cortactin and a cortactin mutant $Cort_{F421F466F482}$, which is deficient in tyrosine phosphorylation [20]. To ensure that most cells express GFP-cortactin proteins, infected cells were sorted based on GFP expression by a flow cytometry system. After sorting, 80% cells exhibited green as analyzed by fluorescent microscopy, and expression levels of GFP-cortactin proteins were comparable with that of endogenous cortactin (Figure 5). The GFP-wt-cortactin behaves similarly as the endogenous cortactin because it can be phosphorylated as efficiently as the

endogenous cortactin in response to H_2O_2. In contrast, GFP-$Cort_{F421F466F482}$ mutant was unable to respond to H_2O_2 for phosphorylation, which confirms our previous conclusion that Tyr421, Tyr466 and Tyr482 are the primary sites for Src in vivo [20].

The cells expressing different forms of GFP-cortactin variants exhibited differential responses to H_2O_2. The GFP-wt-cortactin expressors developed significant membrane blebbing as early as 30 min after treatment (Figure 6A, e and h). Because the similar change in control cells expressing the virus vector was not observed until 1 h after treatment, overexpression of GFP-wt-cortactin appeared to enhance the susceptibility of cells to H_2O_2. In contrast, cells expressing $Cort_{F421F466F482}$ showed little difference in morphology compared to untreated cells either by 30 min or by 1 h treatment (Figure 6A, f and i). Quantitative analysis by counting numbers of cells with membrane blebbing further indicated that overexpression of GFP-$Cort_{F421F466F482}$ can inhibit H_2O_2-induced shape changes by more than 50%, whereas overexpression of GFP-wt-cortactin enhanced the response to H_2O_2 by 20% (Figure 6B).

The activities of cortactin variants were also evaluated in NIH 3T3 cells stably transfected with myc-tagged cortactin variants [20]. Unlike endothelial cells, NIH 3T3 cells did not develop significant membrane blebs in response to H_2O_2 (Figure 7B). Like endothelial cells, however, overexpression of myc-cortactin enhanced the response of NIH 3T3 cells to H_2O_2 because the expressors could develop a dramatic shape change as characterized by rounding up and aggregation either in the presence of H_2O_2 plus PD098059 or H_2O_2 alone at 200 μM, the conditions under which control cells did not exhibit these changes. In contrast to cells expressing myc-cortactin, no significant changes were observed with cells overexpressing Myc-$Cort_{F421F466F482}$ in the presence of either H_2O_2 alone or H_2O_2 plus PD098059. This data confirms

that overexpression of cortactin enhances H_2O_2-induced shape changes in a tyrosine phosphorylation dependent manner.

DISCUSSION

In this study, we provide evidence that tyrosine phosphorylation of cortactin is required for H_2O_2-induced shape changes in human endothelial cells. First, either H_2O_2 alone at high concentrations (more than 1.6 mM) or H_2O_2 at low concentrations (50 to 100 μM) in the presence of PD098059, a selective inhibitor for Erk, induces a significant increase in tyrosine phosphorylation of cortactin. Tyrosine phosphorylation of cortactin appears to be one of the major events induced by H_2O_2, as indicated by analyzing total phosphotyrosyl proteins (Figure 1). Second, the level of tyrosine phosphorylation of cortactin is correlated with the shape changes induced by H_2O_2. The conditions that induce high levels of tyrosine phosphorylation of cortactin are also able to induce shape changes of endothelial cells. These conditions include high concentration (greater than 1.6 mM) of H_2O_2 , H_2O_2 plus PD098059, and H_2O_2 plus vanadate. In addition, tyrosine phosphorylation induced by H_2O_2 is time-dependent and plateaus at 45 min (Figure 2C). This kinetics of tyrosine phosphorylation of cortactin is also correlated with shape changes induced by H_2O_2 (data not shown). Third, tyrosine phosphorylation of cortactin is dependent upon the activity of Src. Treatment of cells with a selective Src inhibitor PP2 can abrogate tyrosine phosphorylation of cortactin as well as the shape changes induced by H_2O_2 (Figure 3). Finally, overexpression of a cortactin mutant deficient in tyrosine phosphorylation can significantly inhibit shape changes induced by H_2O_2 either in endothelial cells or in NIH 3T3 cells (Figure 6 and 7).

Cortactin, a prominent substrate of Src, is a potent filament actin binding protein. In vitro, cortactin also exhibits a potent activity to cross link actin filaments into a filamentous meshwork [21]. Importantly, this F-actin cross-linking activity can be down regulated upon tyrosine phosphorylation mediated by Src. Thus, tyrosine phosphorylation of cortactin likely constitutes

an important mechanism by which Src or its-related protein tyrosine kinases regulate the dynamics of the actin cytoskeleton. In consistent with the role of tyrosine phosphorylation of cortactin in cell shape changes, cells such as Src-/- cells in which cortactin is deficient in tyrosine phosphorylation are more resistant to shape changes induced by extracellular stimuli compared to cells with elevated tyrosine phosphorylation of cortactin [19]. Conversely, cells overexpressing wild-type cortactin acquired a higher sensitivity to shape-change signals such as H_2O_2 (Figure 6 and 7).

Upon exposure to H_2O_2, many endothelial cells develop extensive membrane blebs. Similar morphological changes were also observed in cells expressing high levels of cortactin. For example, tumor cells with high levels of cortactin expression due to gene amplification often develop large spherical membrane protrusions (Ed Schuuring, personal communication). Furthermore, transient transfection of GFP-wt-cortactin, which led to expression of extreme high levels of expression, can also result in apoptotic-like membrane blebbing (Zhan, unpublished result). Membrane blebbing may involve a mechanism similar to the formation of membrane protrusions, lamellipodia and filopodia [27]. In normal cells, cortactin is mainly associated with cell cortical structures, including lamellipodia, membrane ruffles and punctate-like protrusions. Within these structures, cortactin co-localizes with F-actin [20;26]. We found that H_2O_2-induced blebs are rich in cortactin (Figure 3), suggesting that locally concentrated cortactin may be implicated in the formation of membrane blebs. The primary driving force to form membrane protrusions is the actin polymerization occurred underneath the plasma membrane [28]. One possibility is that cortactin could be directly implicated in actin polymerization. Evidence to support this possibility is our recent finding that cortactin is a potent activator of Arp2/3, a protein complex that is responsible for the nucleation of actin polymerization [29]. Cortactin may

also contribute to membrane blebbing through its regulation of F-actin cross-linking. It has been postulated that the flow of the cortical actin gel is a determining factor in the formation of membrane blebs [7]. The rate of flow of the actin gel is inversely regulated by the activity of F-actin cross-linking proteins. Thus, tyrosine phosphorylated cortactin, which has a significant lower F-actin cross-linking activity than non-phosphorylated cortactin [18], would increase the flow of the actin gel and eventually favor a tuned balance toward the formation of membrane blebs. Indeed, human melanoma cell lines deficient in an actin filament cross-linking protein, ABP-280, show prolonged and extensive membrane blebbing [7].

The effect of H_2O_2 on the shape changes in endothelial cells can be dramatically enhanced by PD098059, a chemical that specifically inhibits the activity of Erk 1/2. However, the role of activation of Erk in the oxidant-mediated injury of endothelial cells is not clear. Because the activation of Erk is implicated in the signal pathways of growth factors, Erk may represent a survival factor for cells to antagonize the effect of H_2O_2 [16]. While our data appears to be consistent with this view, we did not find an intimate correlation of the activity of Erk either with phosphorylation of cortactin nor with shape changes. Exposure to H_2O_2 at high concentrations or H_2O_2 at low concentrations in the presence of vanadate can increase tyrosine phosphorylation of cortactin and shape changes as well (Figure 4, and Li, unpublished data). These treatments also induce significant increase in the activity of Erk (Figure 4). Thus, inhibition of Erk by PD098059 is not necessary either for the H_2O_2-mediated tyrosine phosphorylation of cortactin or for cell shape changes. It appears that inhibition of Erk only affects tyrosine phosphorylation of cortactin when low concentration of H_2O_2 is used. One explanation is that lower activity of Erk favors the Src-mediated phosphorylation of cortactin. Evidence to support this argument is that the activity of Erk is reversely correlated with levels of

tyrosine phosphorylation of cortactin when cells are treated with H_2O_2 at 100 μM (data not shown). Because the signal pathway to activate Erk is also regulated by Src [30], it is possible that inhibition of this pathway would make Src more accessible to other substrates, including cortactin.

In summary, our results demonstrate an important role of Src and cortactin in H_2O_2-induced shape changes of endothelial cells. The future studies using small antagonists for cortactin may reveal a novel approach to target specifically at the actin cytoskeleton and protect endothelium from reactive oxygen species.

Reference

1. Hull, D. S., Green, K., Thomas, L., and Alderman, N. (1984) *Invest Ophthalmol.Vis.Sci.* **25,** 1246-1253

2. Schror, K., Thiemermann, C., and Ney, P. (1988) *Naunyn Schmiedebergs Arch.Pharmacol.* **338,** 268-274

3. Sacks, T., Moldow, C. F., Craddock, P. R., Bowers, T. K., and Jacob, H. S. (1978) *J.Clin.Invest* **61,** 1161-1167

4. Orr, F. W., Wang, H. H., Lafrenie, R. M., Scherbarth, S., and Nance, D. M. (2000) *J.Pathol.* **190,** 310-329

5. Nakamura, H., Nakamura, K., and Yodoi, J. (1997) *Annu.Rev.Immunol.* **15,** 351-369

6. Hinshaw, D. B., Sklar, L. A., Bohl, B., Schraufstatter, I. U., Hyslop, P. A., Rossi, M. W., Spragg, R. G., and Cochrane, C. G. (1986) *Am.J.Pathol.* **123,** 454-464

7. Cunningham, C. C. (1995) *J.Cell Biol* **129,** 1589-1599

8. Hastie, L. E., Patton, W. F., Hechtman, H. B., and Shepro, D. (1998) *J.Cell Biochem.* **68,** 511-524

9. Peus, D., Vasa, R. A., Meves, A., Pott, M., Beyerle, A., Squillace, K., and Pittelkow, M. R. (1998) *J.Invest Dermatol.* **110,** 966-971

10. Berk, B. C. (1999) *Thromb.Haemost.* **82,** 810-817

11. Natarajan, V., Scribner, W. M., Al Hassani, M., and Vepa, S. (1998) *Environ.Health Perspect.* **106,** 1205-1212

12. Abe, J., Takahashi, M., Ishida, M., Lee, J. D., and Berk, B. C. (1997) *J.Biol.Chem.* **272,** 20389-20394

13. Carbajal, J. M. and Schaeffer, R. C., Jr. (1998) *Biochem.Biophys.Res.Commun.* **249,** 461-466

14. Barchowsky, A., Munro, S. R., Morana, S. J., Vincenti, M. P., and Treadwell, M. (1995) *Am.J.Physiol* **269,** L829-L836

15. Guyton, K. Z., Liu, Y., Gorospe, M., Xu, Q., and Holbrook, N. J. (1996) *J.Biol.Chem.* **271,** 4138-4142

16. Guyton, K. Z., Liu, Y., Gorospe, M., Xu, Q., and Holbrook, N. J. (1996) *J.Biol Chem* **271,** 4138-4142

17. Zhan, X., Haudenschild, C. C., Ni, Y., Smith, E., and Huang, C. (1997) *Blood* **89,** 457-464

18. Huang, C., Ni, Y., Gao, Y., Wang, T., Haudenschild, C. C., and Zhan, X. (1997) *J.Biol.Chem.* **272,** 13911-13915

19. Liu, J., Huang, C., and Zhan, X. (1999) *Oncogene* **18,** 6700-6706

20. Huang, C., Liu, J., Haudenschild, C. C., and Zhan, X. (1998) *J.Biol.Chem.* **273,** 25770-25776

21. Zhan, X., Hu, X., Hampton, B., Burgess, W. H., Friesel, R., and Maciag, T. (1993) *J.Biol.Chem.* **268,** 24427-24431

22. Wu, H., Reynolds, A. B., Kanner, S. B., Vines, R. R., and Parsons, J. T. (1991) *Mol.Cell Biol.* **11,** 5113-5124

23. Huot, J., Houle, F., Rousseau, S., Deschesnes, R. G., Shah, G. M., and Landry, J. (1998) *J.Cell Biol* **143,** 1361-1373

24. Cuenda, A., Rouse, J., Doza, Y. N., Meier, R., Cohen, P., Gallagher, T. F., Young, P. R., and Lee, J. C. (1995) *FEBS Lett.* **364,** 229-233

25. Alessi, D. R., Cuenda, A., Cohen, P., Dudley, D. T., and Saltiel, A. R. (1995) *J.Biol Chem* **270,** 27489-27494

26. Wu, H. and Parsons, J. T. (1993) *J.Cell Biol.* **120,** 1417-1426

27. Hagmann, J., Burger, M. M., and Dagan, D. (1999) *J.Cell Biochem.* **73,** 488-499

28. Mitchison, T. J. and Cramer, L. P. (1996) *Cell* **84,** 371-379

29. Uruno T, Liu, J, Zhang, B, Fan, X, and Zhan, X. (2000) (submitted)

30. Aikawa, R., Komuro, I., Yamazaki, T., Zou, Y., Kudoh, S., Tanaka, M., Shiojima, I., Hiroi, Y., and Yazaki, Y. (1997) *J.Clin.Invest* **100,** 1813-1821

LEGENDS

Figure 1. H_2O_2 induces protein tyrosine phosphorylation in endothelial cells.

Confluent HUVE cells were exposed to H_2O_2 for 1 h. Prior to H_2O_2, cells were pre-treated with combinations of PP2, PD098059 and SB203580 for either 20 min (for PP2) or 1 h (for PD098059 and SB203580), as indicated. The concentrations of the chemicals used in this experiment were: H_2O_2, 200 μM; PP2, 20 μM; PD098059, 50 μM; and SB203580, 10 μM. After treatments, cell lysates were subjected to immunoblot analysis using a pTyr monoclonal antibody (4G10). The blot was stripped and re-probed with a cortactin monoclonal antibody (4F11).

Figure 2. Tyrosine phosphorylation of cortactin in endothelial cells.

(A). HUVE cells were treated with H_2O_2 at different concentrations for 1 h. The cell lysates were immunoprecipitated with a cortactin polyclonal antibody and then immunoblotted with pTyr (4G10) or cortactin (4F11) antibodies. **(B)**. HUVE cells were pretreated with 100 μM of PD098059 for 1 h and then with H_2O_2 at various concentrations. **C**. HUVE cells were treated with H_2O_2 and PD098059 for the times as indicated and then subjected to phosphotyrosine analysis as above.

Figure 3. H_2O_2 induces morphological changes of endothelial cells.

(A). Microscopic analysis of HUVE cells. Cells grown on fibronectin-coated glass cover slips were pretreated with 0.2% DMSO (a-d) or 100 μM PD098059 (e-h) for 1 h, or 20 μM PP2 (g and h) for 20 min. The cells were further added with 100 μM H_2O_2 (c-h) for 1 h. Treated cells were then stained with either a rhodamine-conjugated cortactin antibody (a, c, e and g) or FITC-conjugated phalloidin (b, d, f, and h). The stained cells were visualized by confocal fluorescent microscopy. **(B)**. Quantification of H_2O_2-induced shape changes. Treated cells with apparent shape changes as characterized by forming membrane blebbing and shrank cytoplasm were

counted under a fluorescent microscope. The means ± standard deviation from three independent experiments is shown.

Figure 4. Inhibition of MAP kinase activity is not necessary for H_2O_2-mediated injury of endothelial cells.

HUVE cells were pretreated with 100 μM PD098059 for 1 h and then added with 100 μM H_2O_2 for 10 min. In addition, cells were treated with pervanadate (the mixture of vanadate and H_2O_2) for 10 min (lane 6). The activity of MAPK was analyzed, as described in the section of Methods and Procedure.

Figure 5. Analysis of tyrosine phosphorylation of GFP-cortactin variants in HUVE cells. HUVE cells were infected with viruses encoding GFP-wt-cortactin, GFP-$Cort_{F421F466F482}$ and GFP only as described in the Methods and Experimental Procedures. Infected cells were pretreated with either DMSO (0.2%) or PD098059 (100μM) for 1 h followed by treatment with H_2O_2 (100μM) for an additional 1 h. The cells were lysed, immunoprecipitated with a cortactin antibody and immunoblotted with a monoclonal phosphotyrosine antibody. The same blot was stripped and reprobed with a monoclonal cortactin antibody (4F11). The positions for GFP-cortactin and endogenous cortactin were indicated.

Figure 6. Analysis of cell shape changes in endothelial cells expressing GFP-cortactin variants. (**A**): HUVE cells were infected with GFP-cortactin viruses as described in the legend of Figure 5. The infected cells were examined under a fluorescent microscope. a, d and g, GFP only; b, e and h, GFP-wt-cortactin; c, f and i, GFP-$Cort_{F421F466F482}$. a-c, without treatment; d-f, treated with H_2O_2 /PD098059 for 30 min; and g-I, treated with H_2O_2/PD098059 for 1 h. (**B**). Cells with membrane blebbing were counted under a microscope. The value for each treatment represents means of three independent experiments.

Figure 7. Overexpression of wild-type cortactin potentiates the response of NIH/3T3 cells to H_2O_2-mediated shape changes.

(A). Stable NIH/3T3 transfectants expressing myc-wt-cortactin and myc-$Cort_{F421F466F482}$ were analyzed for the expression of myc-cortactin proteins by immunoblotting total lysates using monoclonal antibody 9E10 against the myc epitope. Lane 1, cells expressing vector only; lane 2, cells expressing myc-wt-cortactin and lane 3, cells expressing myc-$Cort_{F421F466F482}$. **(B)**. NIH/3T3 transfectants expressing myc-cortactin variant as indicated were grown on fibronectin-coated glass cover slips and treated for 1 h with either 0.2% DMSO as control or 100 μM PD098059. The cells were then treated with H_2O_2 at concentrations as indicated. The cells were inspected under a phase-contrast light microscope.

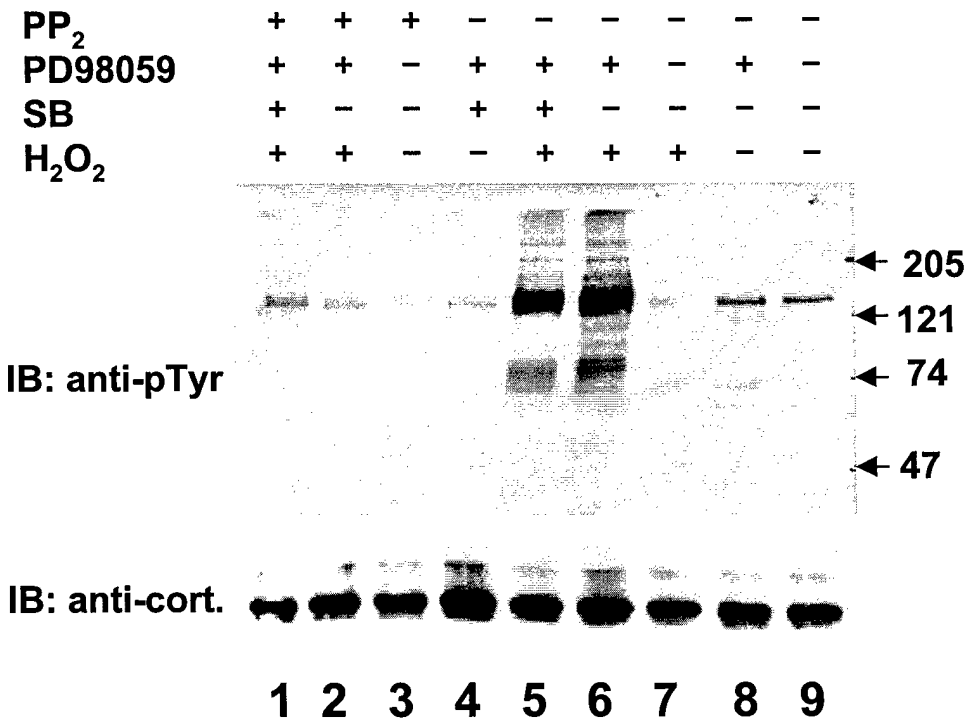

Figure 1, Li et al.

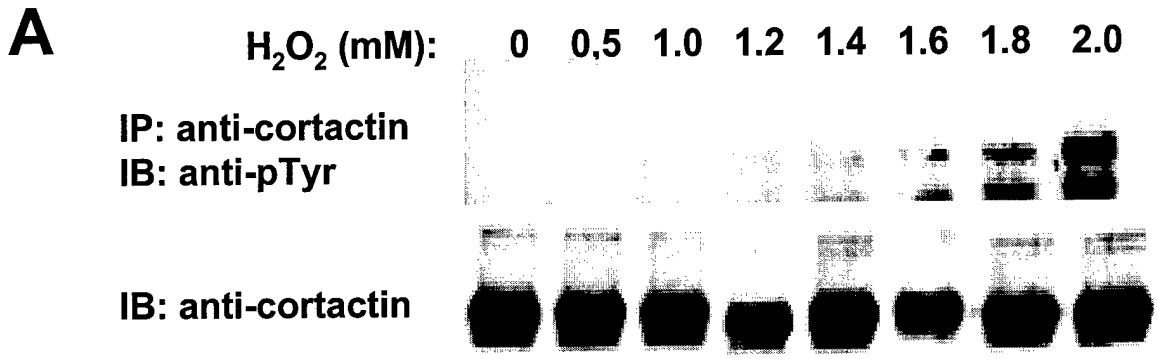

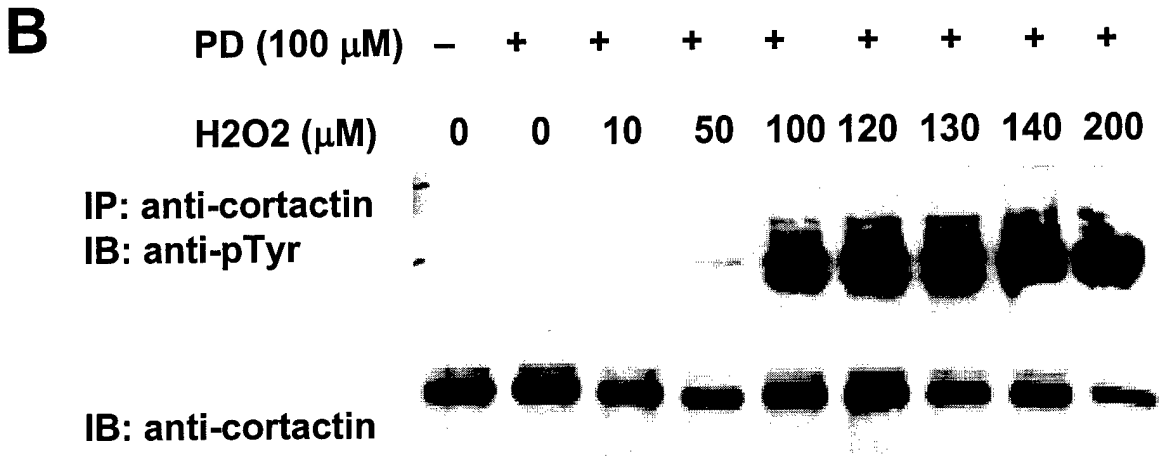

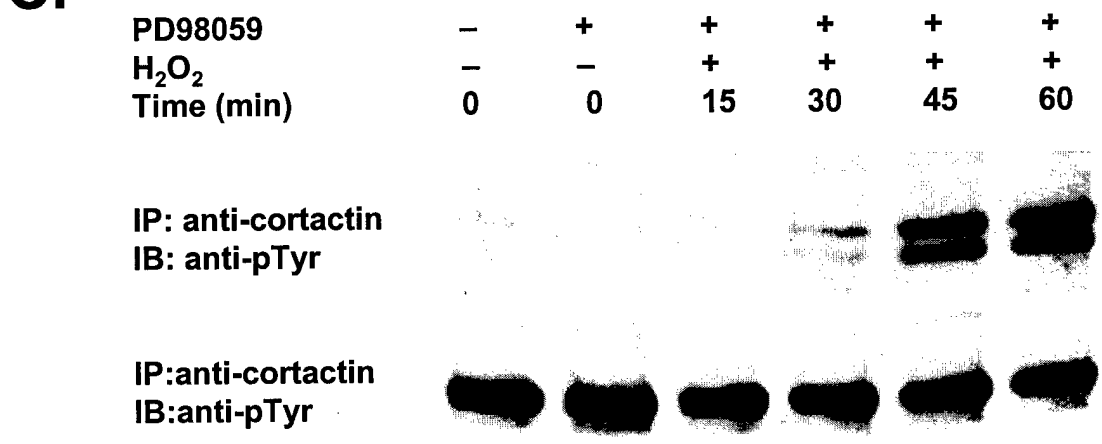

Figure 2, Li et al

A

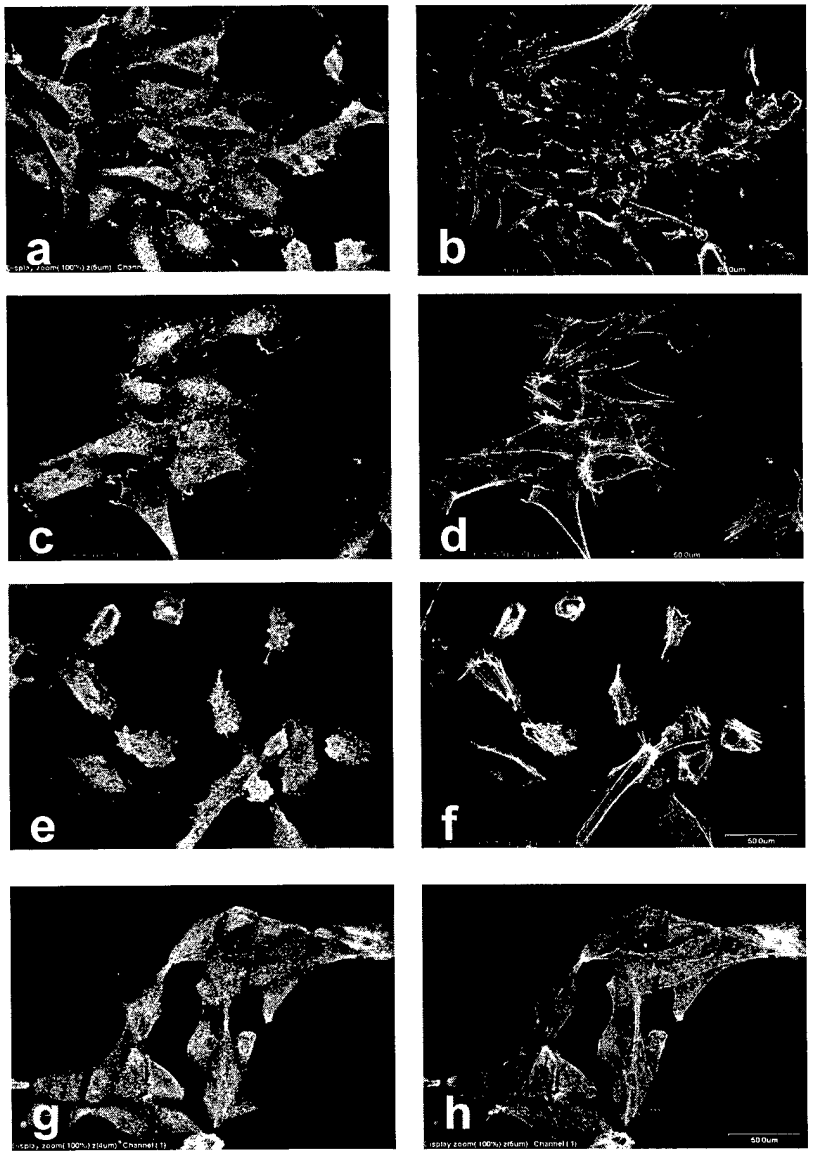

B

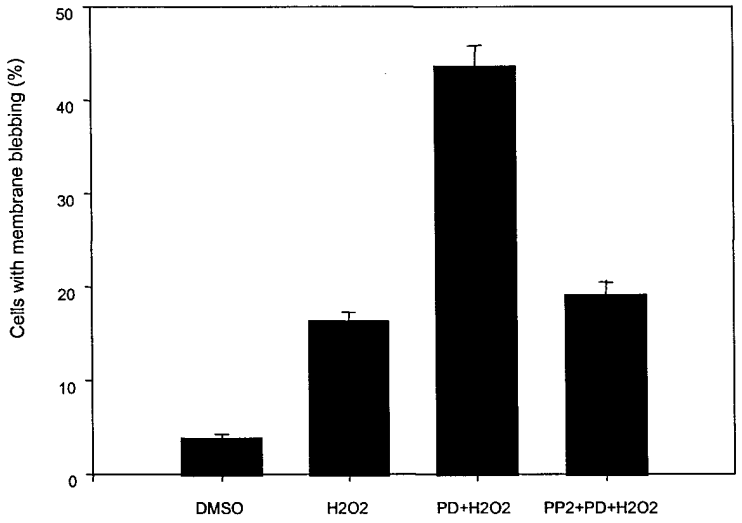

Figure 3
Li, et al

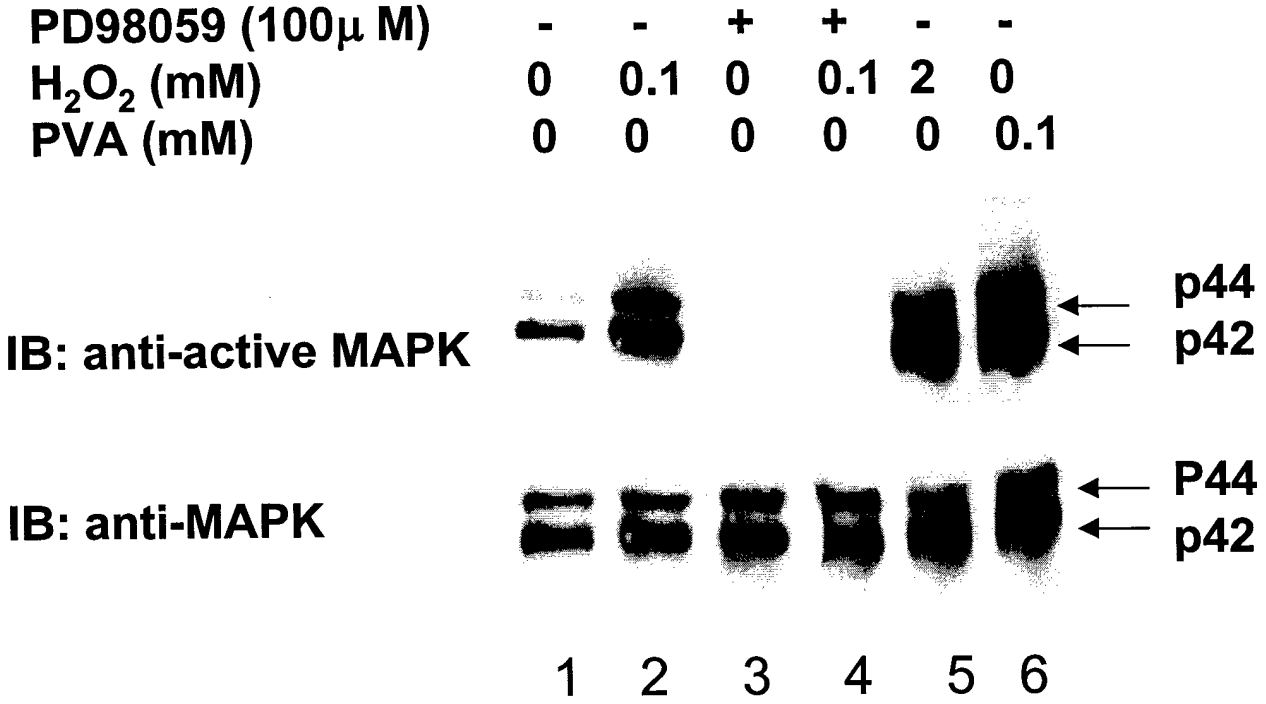

Figure 4, Li, et al

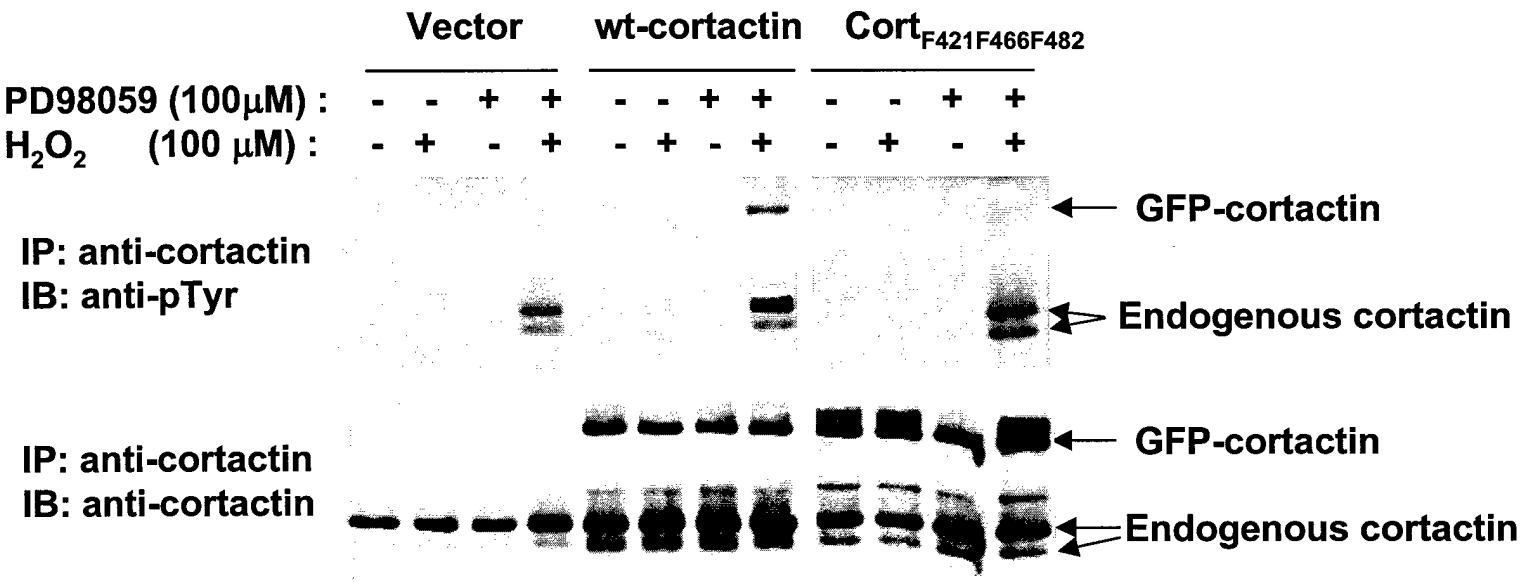

Figure 5, Li et al

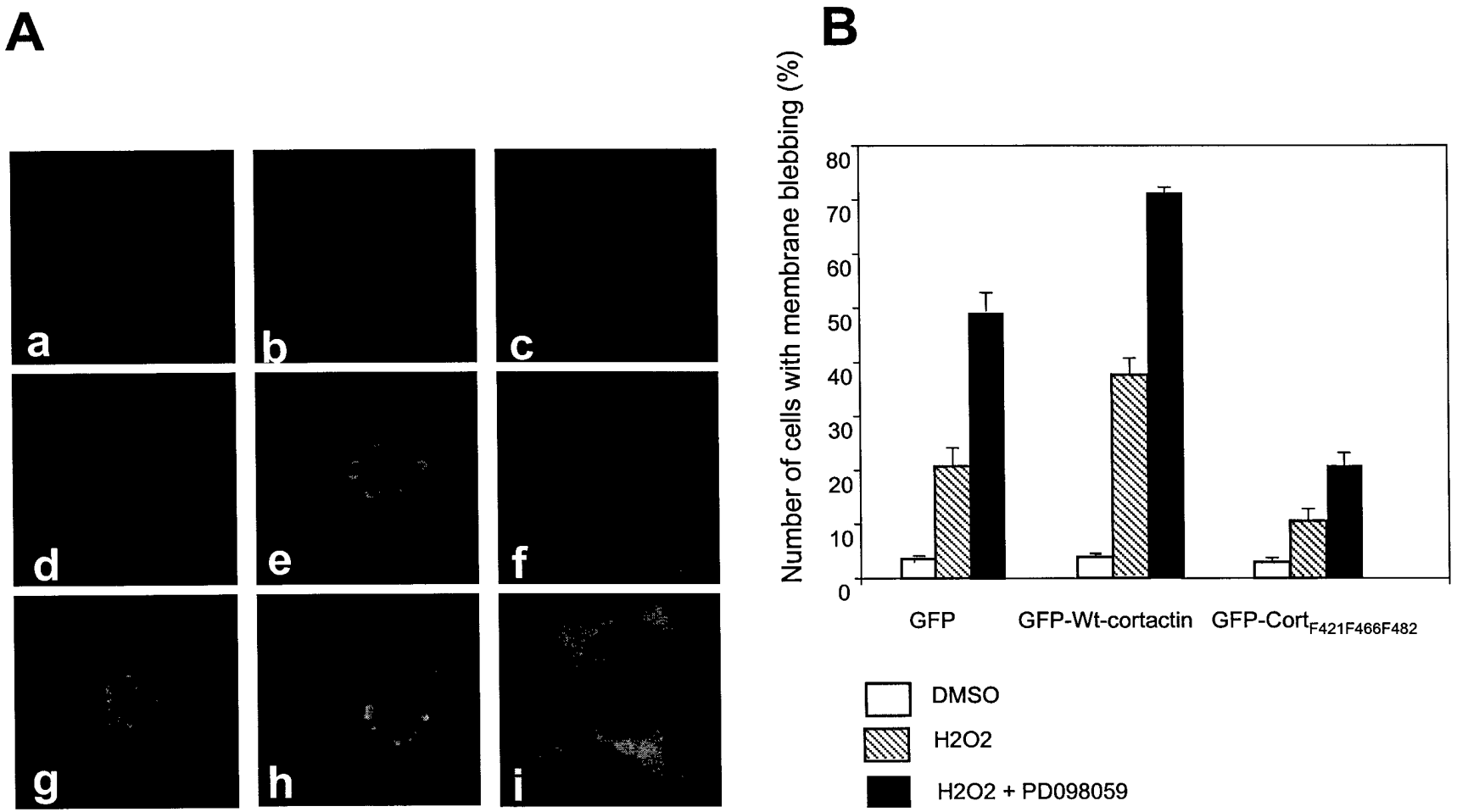

Figure 6, Li, et al.

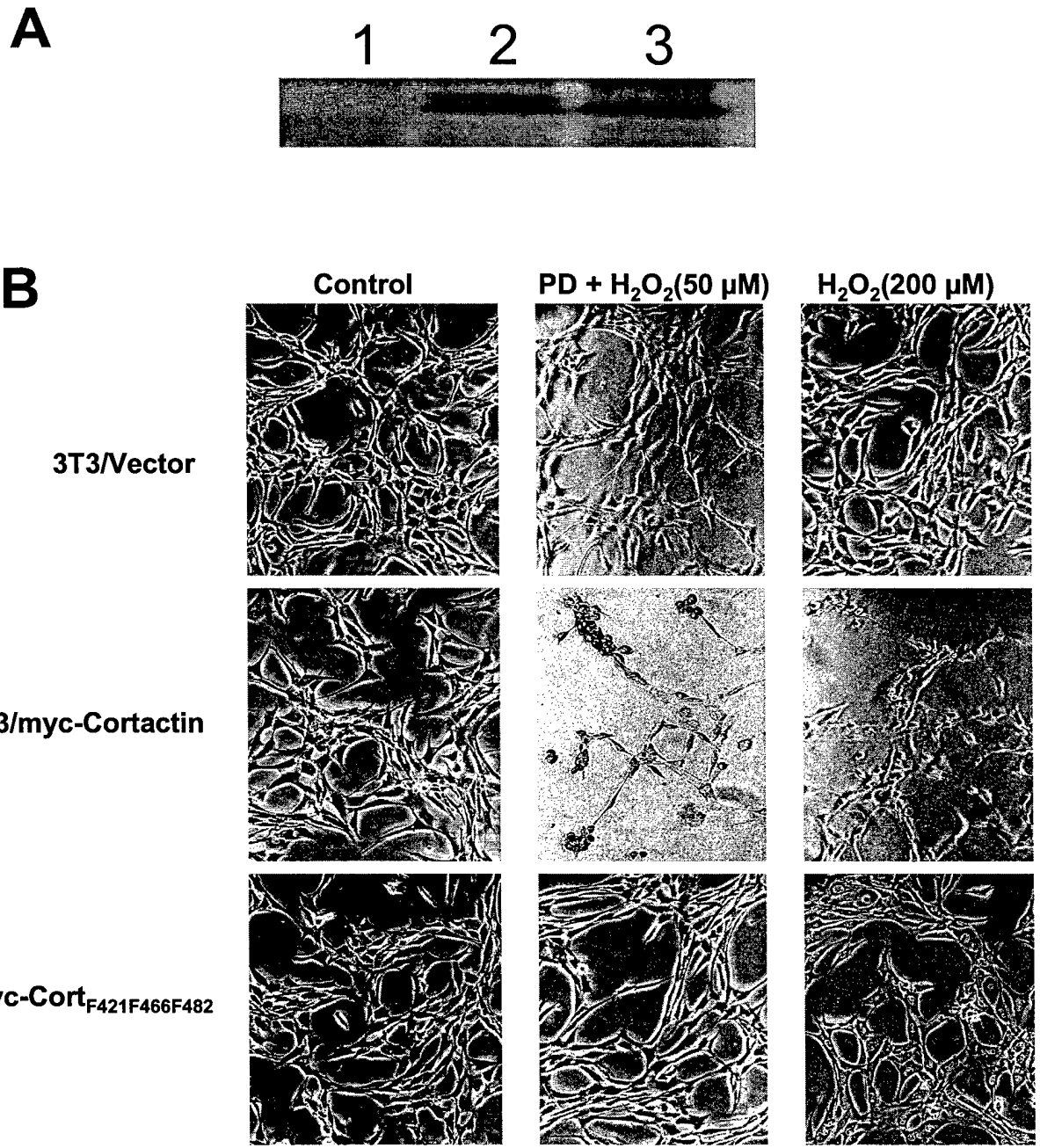

Figure 7, Li et al